

# An investigation into the shear strength of SFRC beams with opening in web using NFEM

Mohammad Karimi\* and Seyed Hamid Hashemi<sup>a</sup>

Department of Civil Engineering, Arak University, Arak, Iran

(Received June 11, 2017, Revised January 11, 2018, Accepted January 26, 2018)

**Abstract.** Making a transverse opening in concrete beams in order to accommodate utility services through the member instead of below or above of that, sometimes may be necessary. It is obvious that inclusions of an opening in a beam decreases its flexural and shear strengths. Fabricated steel bars are usually used to increase the capacity of the opening section, but details of reinforcements around the opening are dense and complex resulting in laborious pouring and setup process. The goal of this study was to investigate the possibility of using steel fibers in concrete mixture instead of complex reinforcement detailing order to strengthen opening section. Nonlinear finite element method was employed to investigate the behavior of steel fiber reinforced concrete beams. The numerical models were validated by comparison with experimental measurements tested by other investigators and then used to study the influence of fiber length, fiber aspect ratio and fiber content on the shear performance of SFRC slender beams with opening. Finally, it was concluded that the predicted shear strength enhancement is considerably influenced by use of steel fibers in concrete mixture but the effect of fiber length and fiber aspect ratio wasn't significant.

**Keywords:** shear strength; opening; steel fiber; RC beam; finite element method

## 1. Introduction

Transverse openings through beams with different shapes and sizes are often provided for essential services and accessibility and are generally located close to the supports where shear is dominant. Among them, circular and rectangular openings are the most common ones in practice (Prentzas 1968). With regard to the size, openings are classified as either large or small. When the opening is little enough to maintain the beam-type behavior or in other words, if the usual beam theory applies, then the opening may be termed as small. When beam-type behavior ceases to exist due to the provision of openings, then that may be classified as a large opening (Mansur 1998). Openings having circular, square or nearly square shapes can be considered as small provided that the depth (or diameter) of opening is in a realistic proportion to the beam size, say, about less than 40% of the overall beam depth (Mansur and Tan 1999).

According to Somes and Corley (1974) when a small opening is introduced in the web of a beam, unreinforced in shear, the mode of failure remains essentially the same as that of a solid beam, however, because opening represents a source of weakness, the failure plane always passes through the opening, unless that's very close to support.

Two types of diagonal tension failure are possible for

beams containing a small opening, beam type failure and frame type failure, and they require separate treatment for a complete design. In frame type failure, two independent inclined cracks form in each of the chord members. The applied shear may be distributed between the two chord members in proportion to their cross-sectional area. Knowing the internal forces, each member can be independently designed for shear following the usual procedure for conventional solid beams Nasser *et al.* (1967).

For beams without shear reinforcement containing small openings (beam type failure), Mansur (1998) proposed that the effective depth,  $d$ , in ACI simplified equation (ACI 318-08 1995) be replaced by the net depth,  $d - d_0$  irrespective of vertical and horizontal location of an opening, where  $d_0$  is diameter/depth of an opening.

SFRC can be regarded as composite material formed by a brittle concrete matrix with short dispersed fibers that can debond and slip from the matrix as stated in Luccioni *et al.* (2012). Fibers are added to inhibit propagation of cracks in the matrix which occur due to its low tensile strength. Fiber reinforced concrete specimens, even those with a small fiber volume fraction, retain post-cracking ability to carry loads as reported by Tejchman and Kozicki (2010). Among different types, steel fibers are the most common in concrete applications.

Experimental and numerical investigations have proved the ability of fibers to control development of crack width when the external loads increase, an increase in energy dissipation and ultimate strength and improvement in post-peak behavior in load displacement response (Spinella 2013, Tahenni *et al.* 2016, Abbas *et al.* 2014). Sahoo *et al.* (2012) studied the behavior of SFRC deep beams with large

\*Corresponding author, Msc.

E-mail: mehrabadimk@gmail.com

<sup>a</sup>Ph.D.

E-mail: h-hashemi@araku.ac.ir

opening. They concluded that replacement of conventional reinforcing bars with deformed steel fibers at a volume of 1.5% can be a feasible alternative to the current practice.

Reinforcement detailing around an opening can be complex, in another hand, Eliminating shear reinforcement in RC elements can potentially reduce the congestion of reinforcing bars and construction costs (Spinella *et al.* 2012, Colajanni *et al.* 2012). This paper looks into the performance of SFRC slender beams with small opening under shear failure. The final goal of this study is to investigate the possibility of using steel fibers in concrete mixture in order to increase opening section shear capacity instead of using a complex reinforcement scheme around an opening.

To do this, a FE model for RC and SFRC beams is described first and then verified. At last, validated FE model is used to examine the effect of fiber length, fiber aspect ratio and volumetric percentage on the predicted shear strength of the beams. The results of this study show that adding steel fibers to concrete is an effective strengthening method to enhance the performance of concrete beams with opening.

## 2. Finite element model

Here, FE model used for simulating the behavior of the beams is briefly described. A 2D nonlinear FE model is developed using ABAQUS (2011). Taking advantage of symmetry about the mid-span plane, just a half of the beam is included in the model as a plane stress problem. The vertical load is applied through displacement increments and to avoid convergence difficulties; the explicit dynamics solver ABAQUS/EXPLICIT is employed to perform the nonlinear analyses. In the following subsections, constitutive models, element types and modeling procedures used in this research are described.

## 3. Material behavior

### 3.1 Concrete in tension

Linear tensile stress-tensile strain relationship is considered for conventional concrete in tension up to the value of the concrete tensile strength. The post-peak behavior is modeled as in Gdde *et al.* (2010)

$$\sigma_c(w) = f_t \exp\left(-\frac{f_t}{G_f} w\right) \quad (1)$$

Where  $G_f$  is fracture energy,  $w$  is crack width and  $f_t$  is concrete tensile strength. By adding fibers to a concrete mix, the objective is to bridge discrete cracks providing for some control over the fracture process and increase the fracture energy (Voo and Foster 2003). To realistically evaluate the tensile stress response of SFRC members, the stress due to the tension-softening effect of the concrete matrix should be added to that attained by steel fibers as shown in Fig. 1 and Eq. (2).

$$\sigma_{SFRC} = \sigma_f + \sigma_c \quad (2)$$

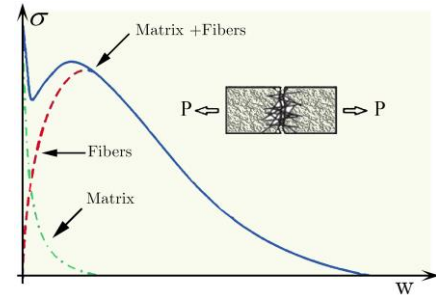


Fig. 1 Stress- displacement diagram

The model proposed by Lee *et al.* (2013) is used to calculate the tensile stress attained by fibers ( $\sigma_f$ ) as Eq. (3) to Eq. (6).

For straight fibers ( $\sigma_f = \sigma_{st}$ )

$$\sigma_{st} = \alpha_f V_f K_{st} \tau_{f,max} \frac{l_f}{d_f} \left(1 - \frac{2w}{l_f}\right)^2 \quad (3)$$

$$K_{st} = \begin{cases} \frac{\beta_f}{3} \cdot \frac{w}{s_f} & w < s_f \\ 1 - \sqrt{\frac{s_f}{w}} + \frac{\beta_f}{3} \sqrt{\frac{s_f}{w}} & w \geq s_f \end{cases} \quad (4)$$

And for the mechanical anchorage of a hooked-end of fiber

$$\sigma_{eh} = \alpha_f V_f K_{eh} \tau_{eh,max} \frac{2(l_i - 2w)}{d_f} \quad (5)$$

$$K_{eh} = \begin{cases} \beta_{eh} \left[ \frac{2}{3} \frac{w}{s_{eh}} - \frac{1}{5} \left(\frac{w}{s_{eh}}\right)^2 \right] & w < s_{eh} \\ 1 + \left(\frac{7\beta_{eh}}{15} - 1\right) \sqrt{\frac{s_{eh}}{w}} - \frac{2(\sqrt{w} - \sqrt{s_{eh}})^2}{l_f - l_i} & s_{eh} \leq w < \frac{l_f - l_i}{2} \\ \left(\frac{l_i - 2w}{2l_i - l_f}\right)^2 K_{eh,i} & \frac{l_f - l_i}{2} \leq w \leq \frac{l_i}{2} \end{cases} \quad (6)$$

So for hooked- end fibers

$$\sigma_f = \sigma_{st} + \sigma_{eh} \quad (7)$$

In above equations  $\alpha_f$  can be assumed to be 0.5,  $V_f$  is volumetric percentage of fibers,  $\beta_f$ ,  $\beta_{eh}$ ,  $s_f$  and  $s_{eh}$  equal to 0.67, 0.76, 0.01 and 0.1 respectively. The frictional bond strength ( $\tau_{f,max}$ ) and the mechanical anchorage strength ( $\tau_{eh,max}$ ) are assumed to be  $0.396\sqrt{f'_c}$  and  $0.429\sqrt{f'_c}$  respectively.

### 3.2 Concrete in compression

The compressive strength, strain corresponding to the failure load and material ductility increase with increasing fiber volume, but the key role of steel fibers is to reduce the rate of strength loss after the peak stress. In this paper, the behavior of SFRC in compression is modeled as in Ezeldin

and Balaguru (1992): Compressive strength of SFRC

$$f'_{SFRC} = f'_c + 3.5RI \quad (8)$$

$$\epsilon_{SFRC} = \epsilon_0 + 446 \times 10^{-6} (RI) \quad (9)$$

Where  $f'_c$  and  $\epsilon_0$  are the compressive stress and strain corresponding to the failure in plain concrete respectively and RI (reinforcing index) equals to

$$RI = W_f \frac{l_f}{d_f} \quad (10)$$

In Eq. (10),  $W_f$  is fiber weight fraction,  $l_f$  is the fiber length and  $d_f$  is fiber diameter. The following equation proposed by Ezeldin and Balaguru (1992) is used to define stress -strain curve

$$\frac{f'_c}{f'_{SFRC}} = \frac{\beta \frac{\epsilon_c}{\epsilon_{SFRC}}}{\beta - 1 + \left( \frac{\epsilon_c}{\epsilon_{SFRC}} \right)^\beta} \quad (11)$$

$$\beta = 1.093 + 0.7132(RI)^{-0.926} \quad \text{hooked end fibers}$$

$$\beta = 1.093 + 7.4818(RI)^{-1.378} \quad \text{Straight fibers}$$

$$\beta = \left( \frac{f'_c}{4.7} \right)^3 + 1.55, f'_c \text{ (ksi)} \quad \text{Plain concrete} \quad (12)$$

Where  $f'_c$ ,  $\epsilon_c$ =stress and strain values on the curve, respectively and  $\beta$  a material parameter.

### 3.3 Steel reinforcement

Steel is assumed identical in tension and compression and an elastic perfectly plastic material. Elastic modulus of 200000 (MPa) and Poisson's ratio of 0.3 are used for the steel reinforcements.

### 3.4 Bond between reinforcement and surrounding concrete

Steel -to- concrete bond is the many-faceted phenomenon, which allows longitudinal force to be transferred from the reinforcement to the surrounding concrete in RC or PC structures. Due to this force transfer, the force in reinforcing bar changes along its length, as does the force in concrete embedment (fib 2000).

Under monotonic loading, two types of bond failures are expected. The first is direct pull-out of the bar, which occurs when large confinement is provided to the bar. The second type of failure is a splitting of the concrete cover when the cover or confinement is insufficient to obtain a pull-out failure (Gan 2000). According to fib (2013), concrete is considered well confined when the ratio of cover to bar diameter is not less than five. In this paper, second type of failure is considered.

In the direction parallel to the steel bar-to-concrete

interface, the properties of the connector elements are defined using the model proposed by reference Harajli *et al.* (1995).

According to this model the relation between local bond stress ( $q$ ) and slip ( $s$ ) of reinforcing bars is defined as below

$$q = q_1 \left( \frac{s}{S_1} \right)^{0.3} \quad s \leq s_c$$

$$q_1 = 31\sqrt{f'_c} \quad (\text{psi}) \quad (13)$$

$$S_1 = 0.15c_0, \quad S_c = S_1 e^{\frac{10 \ln(q_s/q_1)}{3}}$$

Where  $c_0$  is the clear distance between the lugs. The maximum shear stress equals to

$$q_s = \left( 3 + 3.5 \frac{c}{d_b} \right) \sqrt{f'_c} \quad (\text{psi}) \leq q_1 \quad (14)$$

In Equation 14  $c$  and  $d_b$  are clear cover and bar diameter respectively. In SFRC, the post-splitting bond resistance can be calculated as following

$$q_{ps} = 4\sqrt{f'_c} V_f \frac{l_f}{d_f} \left( \frac{c}{d_b} \right) \leq q_s \quad (15)$$

For  $s_c < s < s_3 = c_0$ , shear stress decrease linearly from  $(q_s, s_c)$  to  $(q_{fr}, s_3)$ , and for  $s \geq s_3$  has a constant value equal to  $q_{fr}$  (frictional resistance) =  $0.3q_{ps}$ .

## 4. Material modeling

To simulate concrete response, the damaged plasticity model available in the ABAQUS material library is adopted. Concrete damaged plasticity model provides a general capability for modeling concrete and other quasi brittle materials in all types of structures (beams, trusses, shells, and solids). The model requires that the elastic behavior of the material be isotropic and linear. It assumes that the main two failure mechanisms are compressive crushing and tensile cracking of the material; and cracking initiates at points where the tensile equivalent plastic strain is greater than zero,  $\epsilon_t^{PL} > 0$ , and the maximum principal plastic strain is positive.

The uniaxial tension and compression stress behavior, Poisson's ratio, Young's modulus, the angle of dilation (which controls plastic volumetric strains) the eccentricity  $e$

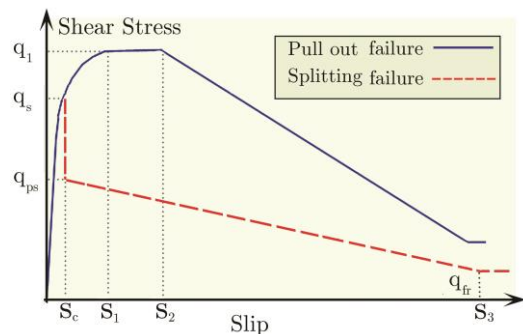


Fig. 2 Local bond stress-slip relationship

Table 1 Assumed values for defining concrete

$E$	$\nu$	$\psi$	$K_c$	$e$	$f_{bo}/f_{co}$
$\frac{0.4f'_c}{\epsilon_c(0.4f'_c)}$	0.2	36	0.5	0.05	1.16

(this parameter can be set equal to zero but adopted value results in easier convergence without any considerable influence on the analysis results), the ratio of equibiaxial to uniaxial compressive stress  $f_{co}/f_{co}$  (it determines the dependency of yield function to hydrostatic pressure) and the ratio of the second stress invariant on the tensile meridian to that on the compressive meridian at initial yield  $K_c$  (this parameter determines the shape of the yield surface on the deviatoric plane, it can vary from 0.5 to 1 changing the shape of the yield surface from triangular to a circle, in this study a simple 2D model is used and low hydrostatic pressure is expected, so the minimum value is adopted) are needed to calibrate the model. In this paper, tensile and compressive behavior, compressive strength and elastic modulus (the slope of a line from origin through the point corresponding to  $0.4f'_c$  c as defined in Mac Gregor (2011)) were modified in order to introduce the effect of steel fibers as described in subsection 3.1 and subsection 3.2. The adopted values for mentioned parameters are presented in Table 1 (all within the range reported in literature).

In order to model the bond behavior between internal longitudinal steel bars and concrete, beam and rebars are meshed in a way that they have coincident nodes. Then connector element is defined between two nodes. In the direction normal to the bars, no relative displacement is allowed between the nodes and the behavior of connector element parallel to the bars is defined based upon the model described in subsection 3.4. Due to the symmetry of the geometry, loadings and boundary conditions, only one-half of the beams are modeled using symmetry boundary conditions in mid-span planes. Concrete beam is simulated using plane stress 4 nodes elements and 2 nodes truss elements were employed to represent the longitudinal reinforcement.

**5. Model validation**

Two sets of experimentally tested RC and SFRC beams

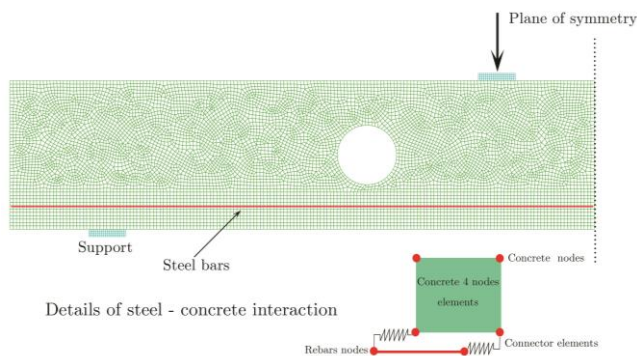


Fig. 3 Finite element model

without stirrups failing in shear are used for model validation. The first set comprised the three beams (control beam, HE-50-0.5, HE-50-0.75) tested by reference Greenough and Nehdi (2008). The beam specimens were 200 (mm)×300 (mm)×2400(mm) in size with a reinforcement ratio of 1.7% and were subjected to 4-point bending (Fig. 4) under the constant shear span to the effective depth ratio  $a/D=3$ . The concrete used had a maximum aggregate size of 10 (mm) and characteristic compressive strength of 40 (MPa) and Standard Grade 400 deformed steel bars were used for the longitudinal reinforcement with a specified yield strength of 400 (MPa).

0.5% and 0.75% hooked end steel fibers of 50 (mm) length and 1 (mm) diameter were used in HE-50-0.5 and HE-50-0.75 beams respectively. The properties of concrete assumed in numerical concrete are summarized in Table 2. Using lower limit of tensile strength led to closer agreement with test results.

The experimental and numerical load-deflection curves of the beams are depicted in Fig. 5. This figure clearly demonstrates that there is an appropriate agreement between the experimental and FE predicted load- deflection behavior from initial loading up to beam failure. Of course for the first beam (control beam), simulated beam is stiffer than experimental beam (note good agreement in ultimate strength), one justification for that can be the specimen sitting that usually happens in experimental tests.

The second set included the three RC beams tested by Pimanmas (2010). Beam “Con-s1” was the control beam without opening. Beams “C-con” and “R-con” were provided with circular and square holes without any

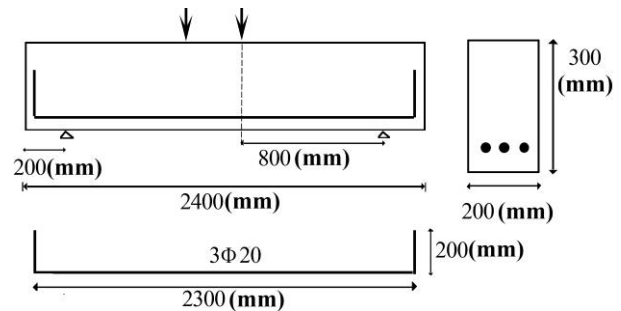
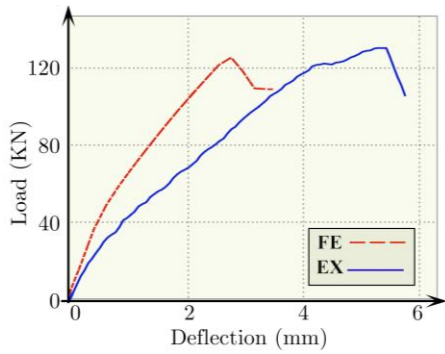


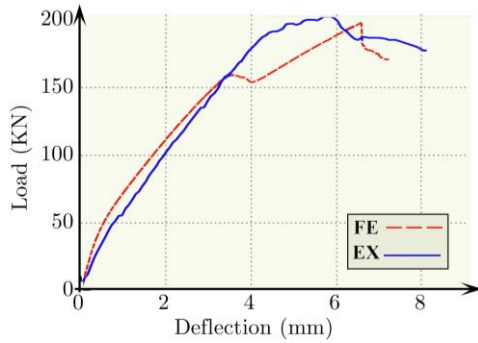
Fig. 4 Schematic of beam dimensions and test setup

Table 2 Assumed concrete characteristics (CEB-FIP MODEL CODE 1990 (1993))

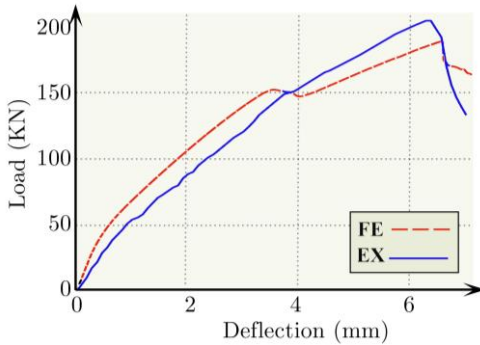
Fracture energy	$G_f (N / m) = 75$
Characteristic compressive strength	$f_{ck} (MPa) = 40$
Mean value of compressive strength	$f_{cm} = f_{ck} + 8 = 48 (MPa)$
Tensile strength (MPa)	
Upper limit	$1.85 \left( \frac{f_{ck}}{10} \right)^{\frac{2}{3}} = 4.68$
mean	$1.4 \left( \frac{f_{ck}}{10} \right)^{\frac{2}{3}} = 3.55$
Lower limit	$0.95 \left( \frac{f_{ck}}{10} \right)^{\frac{2}{3}} = 2.4$



(a)



(b)



(c)

Fig. 5 Experimental and numerical load deflection curves, (a) control beam, (b) S-HE-50-0.5 beam, (c) S-HE-50-0.75 beam

Table 3 Steel bars properties

steel	Yield strength (MPa)	Tensile strength (MPa)
DB20	484	611
RB6	362	490

strengthening. The circular opening had the diameter of 150 (mm) and the square opening was 150 (mm)×150 (mm) in size. The average compressive strength of concrete was 34.1 MPa. The properties of steel bars are given in Table 3.

The details of the beams are shown in Fig. 6.

Fig. 7 and Fig. 8 depict the comparison between experimental and numerical load -deflection curves and crack patterns comprising the control beam “Con-s1” and beams with opening (“C-con” and “R-con”). Comparison indicates that results from the FE models are matched with those from the experiment.

The FE model had predicted/experimental shear strength

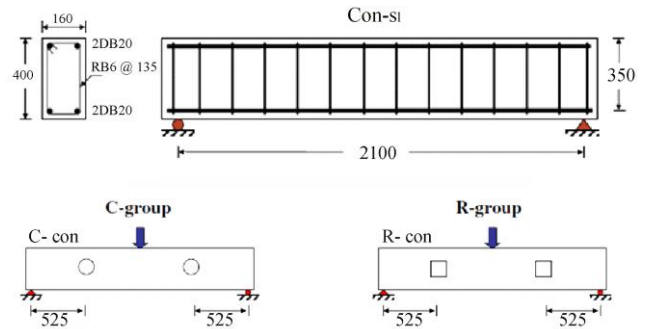
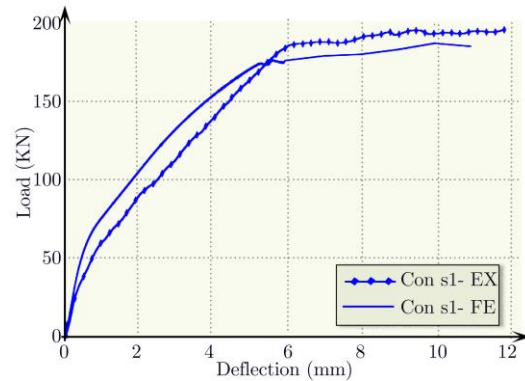
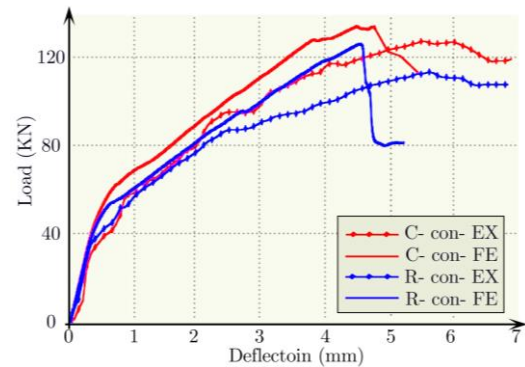


Fig. 6 Dimension of beams and reinforcement details (Pimanmas 2010)



(a)



(b)

Fig. 7 Experimental and numerical load- deflection curves, (a) solid beam, (b) beams with opening

ratio of 0.94, 1.06 and 1.12 for “Con-s1”, “C-con” and “R-con” beams respectively.

## 6. Parametric study

Based on the demonstrated accuracy of the developed FE model, a numerical parametric study was executed to investigate the shear behavior of SFRC beams with small circular opening. The variable parameters included the fiber length (35, 50, 60), fiber aspect ratio (46.6, 50, 60, 63.6; 66.6, 80) and volumetric percentage of fibers (0.5, 1, 1.5%). The details of analytical specimens are shown in Figure 9. Totally, 12 beams with shear span to effective depth ratio  $a/d$  of 3 and longitudinal reinforcement ratio of 1.1% are

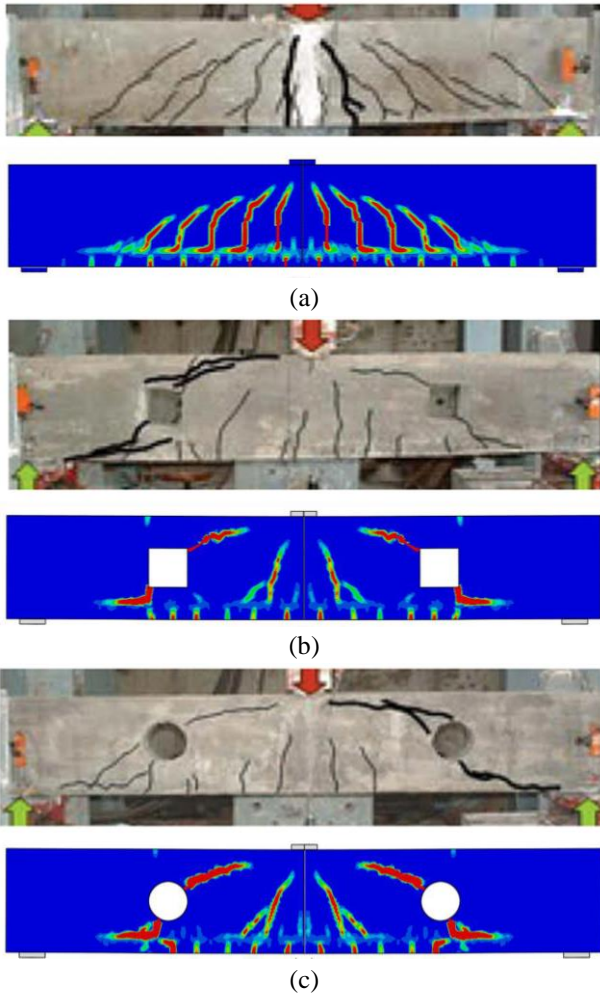


Fig. 8 Experimental and numerical crack patterns, (a) “Coc-S1” beam, (b) “R-con beam”, (c) “C-con” beam

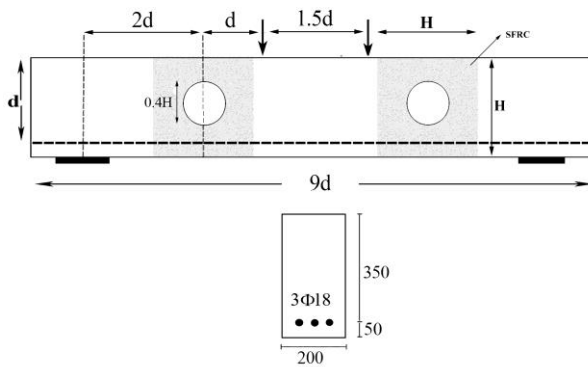


Fig. 9 Details of analytical beams

Table 4 Concrete and steel properties for analytical beams

Concrete characteristic compressive strength	40 (MPa)
Concrete tensile strength	3.55 (MPa)
Maximum aggregate size	16 (mm)
Steel yielding strength	500 (MPa)

analyzed. Details of the beams and Material properties assumed in the analysis are reported in Table 4 and Table 5 respectively.

Table 5 Properties of analytical beams

Beam	Opening	Fiber fraction	Fiber length	Fiber aspect ratio
B-Control	-	-	-	-
B-circle	circle	-	-	-
B-35-0.55-0.5	circle	0.5	35	63.63
B-35-0.75-0.5	circle	0.5	35	46.67
B-35-0.75-1	circle	1	35	46.67
B-35-0.75-1.5	circle	1.5	35	46.67
B-50-1-0.5	circle	0.5	50	50
B-50-0.75-0.5	circle	0.5	50	66.66
B-60-1-0.5	circle	0.5	60	60
B-60-0.75-0.5	circle	0.5	60	80
B-50-1-1	circle	1	50	50
B-50-1-1.5	circle	1.5	50	50

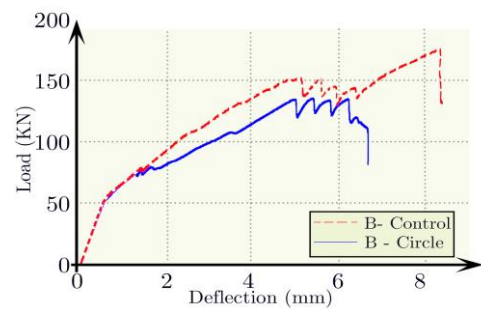


Fig. 10 Load-deflection curves of analytical beams

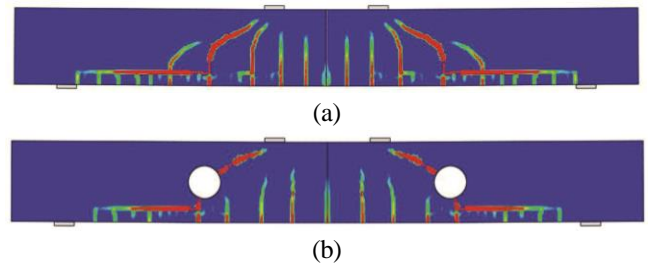


Fig. 11 Predicted crack patterns of analytical beams

## 7. Results

### 7.1 Effect of opening

Fig. 10 depicts the load-deflection of “B-Control” and “B-Circle” beams. Both beams experienced brittle shear failure. The maximum load of beam “B-Control” was 176.8 (KN) while that of beam “B-Circle” was 135.5 (KN). The capacity, drops 23.3% in beam “B-Circle” Compared to the solid control beam.

The predicted crack patterns for these two beams are also shown in Fig. 11. In both beams, the main diagonal crack first starts in approximately distance  $d$  from the loading point and then propagates toward support and loading point simultaneously.

### 7.2 Effect of fibers volumetric percentage

The effect of the steel fibers content is examined in this subsection. Table 6 summarizes maximum applied load,

Table 6 FE results

Beam	Maximum load (KN)	Deflection (mm)	Increase in shear strength over B-circle %
B-control	171.2	8.5	-
B-circle	135.5	5.08	-
B-50-1-0.5	171.2	7.67	20.8
B-50-1-1	215.8	9.3	37.2
B-50-1-1.5	240.6	10.35	43.7
B-35-0.75-0.5	164.8	7.42	17.8
B-35-0.75-1	204.8	8.94	33.8
B-35-0.75-1.5	226.4	9.85	40.1

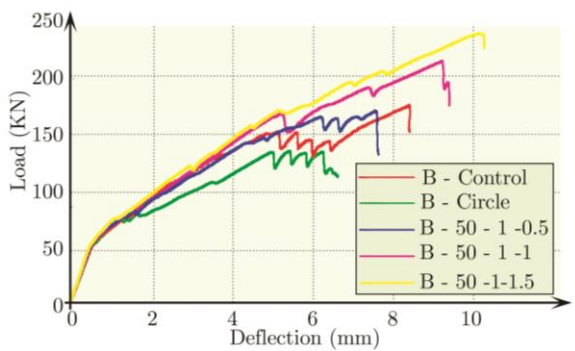


Fig. 12 Effect of fiber content

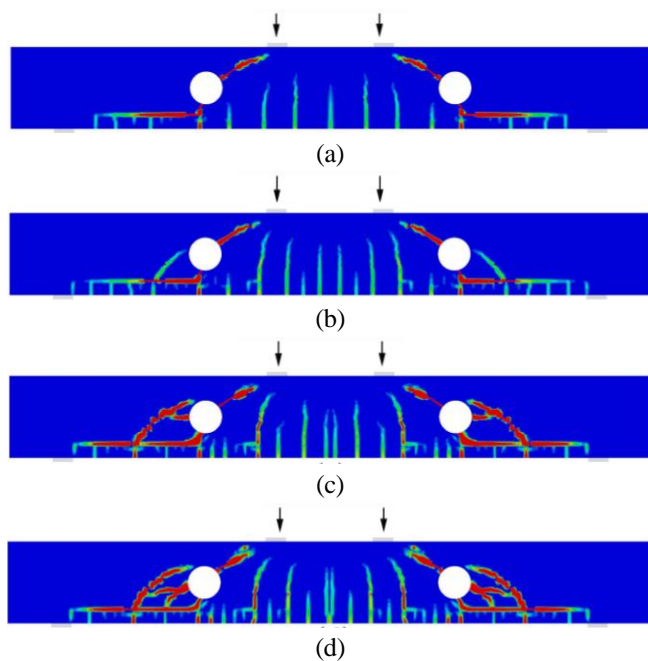
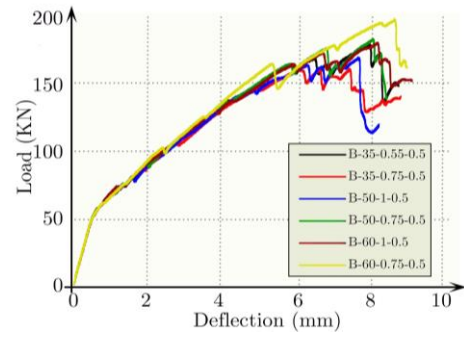


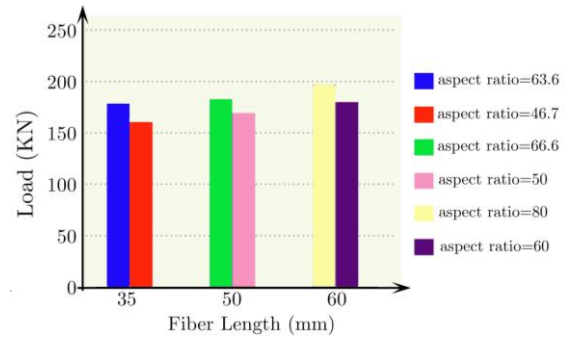
Fig. 13 Predicted crack patterns, (a) “B-circle” beam, (b) B-50-1-0.5 beam, (c) B-50-1-1 beam, (d) B-50-1-1.5 beam

corresponding deflection and the increase in shear strength over that of “B-circle” beam for each analyzed beam specimen in percent. The load-deflection relationships for the various beams are also shown in Fig. 12.

It can be seen that the beams reinforced with 0.5% steel fibers resisted the load approximately equal to the solid beam and beams reinforced with 1% and 1.5% steel fibers resisted over 19% and 32% more load than that of solid beam respectively..



(a)



(b)

Fig. 14 Parametric study, (a) Load deflection curves, (b) Effect of fiber length and fiber aspect ratio on the shear strength

It can be observed in Fig. 12 that all of the SFRC beams failed in shear, but had greater deflection at maximum load and more ductile failure than that of the beams made of plain concrete

The predicted crack patterns are shown in Fig. 13. As it can be seen, there are deeper and closer flexural cracks in SFRC beams in the pure bending region. In the shear span, as the volumetric percentage of fibers increases, more number of cracks pass through the opening.

## 8. Conclusions

In this paper, a FE model for RC & SFRC beams was developed and validated using published experiments from the literature. A parametric study was conducted to investigate the influence of fiber length, fiber aspect ratio and fiber volumetric parentage on the predicted behavior of RC and SFRC beams without stirrups with circular penning. The following conclusions can be drawn from nonlinear FE analyses:

- Introducing a circular opening of 0.4H diameter decreased the shear strength approximately 24% relative to solid beam.
- The opening section using steel bars can be time-consuming and labor-intensive due to the complex detailing of reinforcing bars. Replacement of conventional reinforcing bars with hooked steel fibers was studied. The results showed that beams with 0.5% fiber volume fraction can resist the load approximately equal to solid beam.
- Using more amounts of fibers in the mixture of

concrete considerably increased the capacity of the “B-circle” beam. In average, 74% increase in capacity for 1.5% fiber volume fraction and 55% increase in capacity for 1% fiber volume fraction was achieved. In addition to strength, SFRC beams had more ductile failure mode. Hence, replacement of reinforcing bars with steel fibers seems to be a feasible alternative.

- Despite the fiber volumetric percentage, fiber length had no significant effect in the range studied in this paper (aspect ratio 47 to 80). Having 0.5% fiber content, in the maximum case 4% increase in the capacity was observed. these results are in agreement with those reported in (Yassir and Iqbal Khan 2016) where artificial neural network model was developed to predict the ultimate shear strength of steel fiber reinforced concrete (SFRC) beams without web reinforcement and it was shown that for beams having  $a/d=3.2$  increasing fibers length from 35 (mm) to 60 (mm) resulted in approximately no more shear strength. Fiber aspect ratio had more effect but yet minor as shown in Fig. 14.

## References

- Abbas, A.A., Mohsin, S.M.S. and Cotsovovs, D.M. (2014), “Seismic response of steel fiber reinforced concrete beamcolumn joints”, *Eng. Struct.*, **59**, 261-283.
- Abbas, Y.M. and Iqbal Khan, M. (2016), “Influence of fiber properties on shear failure of steel fiber reinforced beams without web reinforcement: ANN modeling”, *Lat. Am. J. Solid Struct.*, **13**, 1483-1498.
- ACI Committee 318 and American Concrete Institute and International Organization for Standardization (1995), Building Code Requirements for Structural Concrete (ACI 318-08) and Commentary, Beams in Shear, American Concrete Institute, USA.
- Colajanni, P., Recupero, A. and Spinella, N. (2012), “Generalization of shear truss model to the case of SFRC beams with stirrups”, *Comput. Concrete*, **9**(3), 227-244.
- Comite Euro-International Du Beton (1993), *CEB-FIP MODEL CODE 1990*, Thomas Telford Publishing, UK.
- Du Béton, F. (2000), *Bond of Reinforcement in Concrete: State-of-the-Art Report*, International Federation for Structural Concrete.
- Du Beton, fib - Federation Internationale (2013), *fib Model Code for Concrete Structures 2010*, Wiley.
- Ezeldin, A.S. and Balaguru, P.N. (1992), “Normal-and high-strength fiber reinforced concrete under compression”, *J. Mater. Civil Eng.*, **4**(4), 415-429.
- Gan, Y. (2000), “Bond stress and slip modeling in nonlinear finite element analysis of reinforced concrete structures”, Ph.D. Thesis, University of Toronto, Canada.
- Gödde, L., Mark, P., Bićanić, N., de Borst, R., Mang, H. and Meschke, G. (2010), “Numerical modelling of failure mechanisms and redistribution effects in steel fiber reinforced concrete slabs”, *Computational Modelling of Concrete Structures (EURO-C 2010)*, CRC Press, Boca Raton, FL.
- Greenough, T. and Nehdi, M. (2008), “Shear behavior of fiber-reinforced selfconsolidating concrete slender beams”, *ACI Mater. J.*, **105**(5), 468.
- Harajli, M., Hout, M. and Jalkh, W. (1995), “Local bond stress-slip behavior of reinforcing bars embedded in plain and fiber concrete”, *ACI Mater. J.*, **92**(4), 343-353.
- Karlsson, H. and Sorensen Inc. (2011), ABAQUS 6.11 Analysis User’s Manual.
- Lee, S.C., Cho, J.Y. and Vecchio, F.J. (2013), “Simplified diverse embedment model for steel fiber reinforced concrete elements in tension”, *ACI Mater. J.*, **110**(4), 403-412.
- Luccioni, B., Ruano, G., Isla, F., Zerbino, R. and Giaccio, G. (2012), “A simple approach to model SFRC”, *Constr. Build. Mater.*, **37**, 111-124.
- MacGregor, J.G. (2011), *Reinforced Concrete: Mechanics and Design*, Pearson Prentice Hall.
- Mansur, M. (1998), “Effect of openings on the behavior and strength of r/c beams in shear”, *Cement Concrete Compos.*, **20**(6), 477- 486.
- Mansur, M. and Tan, K. (1999), *Concrete Beams with Openings: Analysis and Design*, New Directions in Civil Engineering, CRC Press, USA.
- Nasser, K. W. Acavalos, A. and Daniel, H. (1967), “Behavior and design of large openings in reinforced concrete beams”, *Journal Proceedings*, vol. 64, pp. 25-33.
- Pimanmas, A. (2010), “Strengthening r/c beams with opening by externally installed frp rods: Behavior and analysis”, *Compos. Struct.*, **92**(8), 1957-1976.
- Prentzas, E.G. (1968), “Behavior and reinforcement of concrete beams with large rectangular apertures”, Ph.D. Thesis, University of Sheffield, UK.
- Sahoo, D.R., Flores, C.A. and Chao, S.H. (2012), “Behavior of steel fiber reinforced concrete deep beams with large opening”, *ACI Struct. J.*, **109**(2), 193-203.
- Somes, N. and Corley, W. (1974), “Circular openings in webs of continuous beams”, *ACI Spec. Publ.*, **42**, 359-398.
- Spinella, N. (2013), “Shear strength of full-scale steel fibre-reinforced concrete beams without stirrups”, *Comput. Concrete*, **11**(5), 365-382.
- Spinella, N., Colajanni, P. and La Mendola, L. (2012), “Nonlinear analysis of beams reinforced in shear with stirrups and steel fibers”, *ACI Struct. J.*, **109**(1), 53-63.
- Tahenni, T., Chemrouk, M. and Lecompte, T. (2016), “Effect of steel fibers on the shear behavior of high strength concrete beams”, *Constr. Build. Mater.*, **105**, 14-28.
- Tejchman, J. and Kozicki, J. (2010), *Experimental and Theoretical Investigations of steel fibrous Concrete*, Springer.
- Voo, J.Y. and Foster, D.S.J. (2003), “Variable engagement model for fiber reinforced concrete intension”, University of Sheffield, UK.

HK